ISTITUTO NAZIONALE DI FISICA NUCLEARE
Laboratori Nazionali di Frascati

LNF-77/32(R)
8 Luglio 1977

G. Giordano and G. Matone: LASER LIGHT MODULATION: THE ACOUSTOOPTICAL EFFECT AND THE CAVITY DUMPING TECHNIQUE.

Servizio Documentazione
dei Laboratori Nazionali di Frascati
Cas. Postale 13 - Frascati (Roma)

INFN - Laboratori Nazionali di Frascati
Servizio Documentazione

LNF-77/32(R)
8 Luglio 1977

G. Giordano and G. Matone: LASER LIGHT MODULATION: THE ACOUSTOOPTICAL EFFECT AND THE CAVITY DUMPING TECHNIQUE.

INTRODUCTION. -

As extensively described elsewhere[1], the energy resolution of the Ladon beam can be improved a lot by preventing the electron-photon collisions to take place inside the quadrupole regions of the Adone straight section.

A possible way of doing it is to bunch the laser beam in such a way that photon and electron bunches collide only in the middle of the straight section (see Fig. 1).

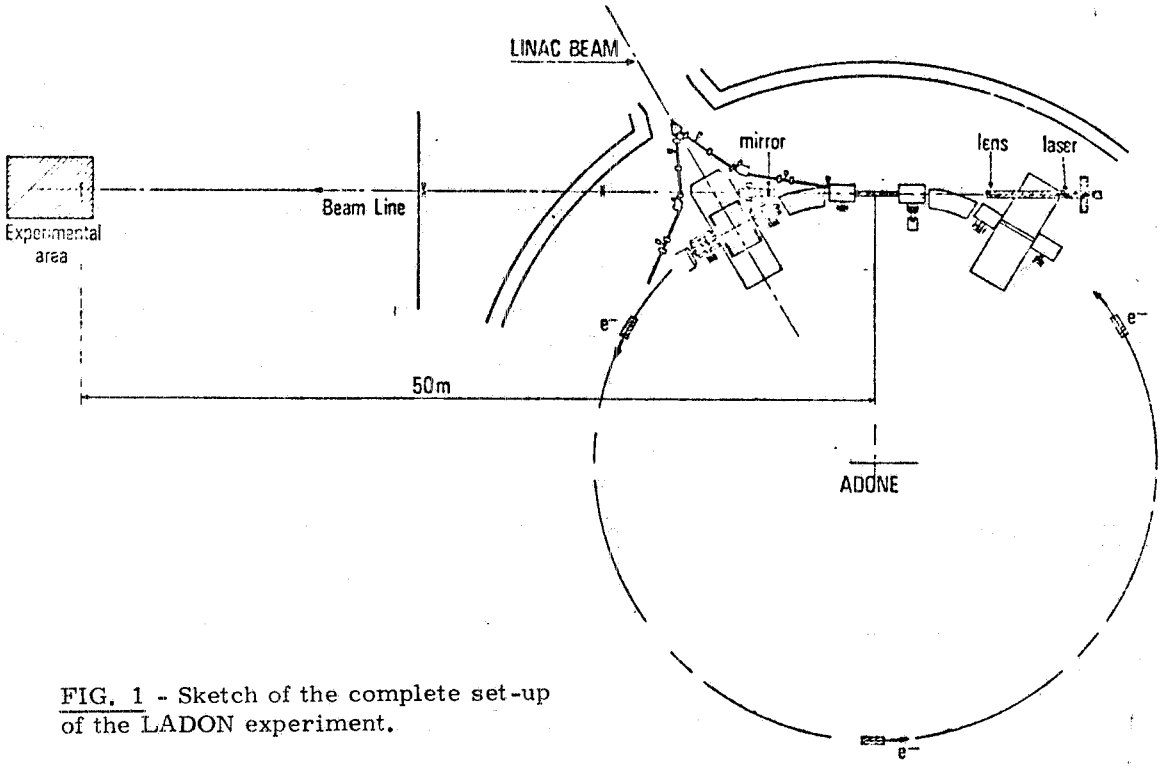

FIG. 1 - Sketch of the complete set-up of the LADON experiment.

This requires to have light pulses with a repetition frequency of 8.5 MHz (Adone RF) and width less than 20 nsec.

This work has been expecially undertaken to analize tha main operating features of the cavity dumping technique. Such a method looks in fact extremely promising since it allows to get laser light pulses with good risetime, high repetition frequency and substantially high peak powers. In particular its appliance to the Spectra Physics 170/03 Argon Ion laser enables to obtain pulses of 100 Watt and consequently suggests that this method can be the proper and definite way to operate the Ladon beam.

We want to stress that this paper is also devoted to present in detail the general performances of this technique whose features have been requested to us in several occasions.

1. - LIGHT-SOUND SCATTERING IN ABSENCE OF VOLUME LOSSES. -

It is well known that ultrasonic waves in transparent materials can be used to deflect or scatter light beams.

With the advent of laser these diffraction phenomena got a great technical importance similar to that of the electrooptic effect[2]. Contrary to this, the elastooptic effect is not confined to the non-centro-symmetrical classes, but occurs throughout the 32 classes and omorphous media as well. So there is a broader variety of materials that could serve for suitable modulators.

This chapter is devoted to show how some of the theoretical results for the light-sound scattering have relevance to laser beam deflection devices and in particular to interpret the main operating features of the laser cavity dumper we will discuss in Section 2.

1.1. - Theoretical generalities.

We will give a brief mathematical treatment of the interaction between a sound wave and a light wave in absence of volume loss. The geometry of the interaction is shown in Fig. 2. The acoustic wave propagates along the x-axis and it is assumed to be confined in the rectangular strip

$$0 \leq Y \leq L$$

where L is the width of the interaction region.

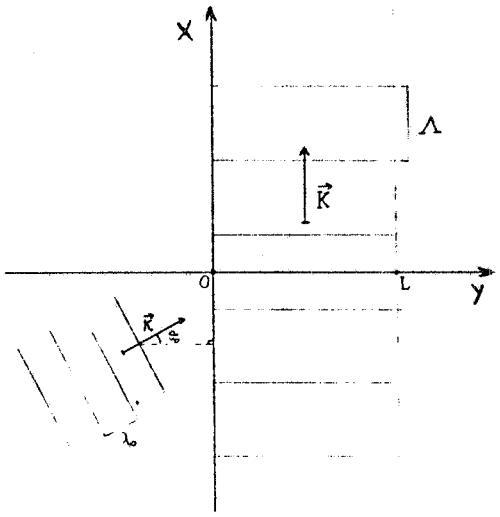

FIG. 2 - Geometry of the interaction region.

The direction of propagation of the light beam lies in the X-Y plane and makes an angle θ_o with the y-axis. Its polarization is parallel to the z-axis and it is assumed that the optical field has no z variation. Furthermore, we assume both the acoustic and optic beams to be plane.

The sound wave produces, via the photoelastic effect, a periodic variation $\Delta\varepsilon$ in the dielectric constant ε_o of the medium, given by[3]:

$$\Delta\varepsilon(x,y,t) = \delta\varepsilon(y)\cos(\Omega t - Kx) \qquad (1)$$

where:

Ω is the acoustic angular frequency,
K is the acoustic momentum ($K = \Omega/v$),
v is the acoustic velocity.

It can be shown that the optical field E (= E_z) with angular frequency ω is described by the wave equation:

$$\frac{\partial^2 E}{\partial X^2} + \frac{\partial^2 E}{\partial Y^2} - \frac{1}{c'^2}\frac{\partial^2}{\partial t^2}\left(1 + \frac{\Delta\varepsilon}{\varepsilon_o}\right)E = 0 \ , \qquad (2)$$

where $c' = c/n$ is the light velocity in the medium.

According to a standard procedure, the perturbed E is expanded in a set of plane waves appropriate to the grating orders associated with a periodic variation of the refraction index n :

$$E(x,y,t) = \sum_{-\infty}^{+\infty}{}_{1}\, V_1(y) \exp i\left[(\omega + 1\Omega)t - (k \operatorname{sen}\theta_o + 1K)x - k\cos\theta_o y\right] + \text{c. c.} \qquad (3)$$

whereas, in absence of the perturbation in the dielectric constant, E is assumed to be a plane wave with propagation constant $k = \omega/c'$. Before solving (2) we observe that (3) represents a superposition of waves of frequency $\omega_1 = \omega + 1\Omega$ ($1 = 0, \pm 1, \pm 2, ..$). Moreover, the x-component of the wave-vector of frequency ω_1 is $k \operatorname{sen}\theta_o + 1K$. Therefore the sine of the angle ϕ_1 that the wave makes with the y-axis inside the scattering medium is[4] :

$$\operatorname{sen}\phi_1 = \frac{c'(k \operatorname{sen}\theta_o + 1K)}{\omega + 1\Omega} \simeq \operatorname{sen}\theta_o + 1\frac{\lambda}{\Lambda} \qquad \left(\text{since } \frac{\Omega}{\omega} << 1\right)$$

where $\lambda\ (= n\lambda_o)$ and Λ are the optic and acoustic wavelengths respectively. Further, the quantity $V_1(y)$ can be identified as the amplitude of the 1-th deflected beam of frequency ω_1.

Substituting (3) into (2) yields, after performing the required algebra, a set of equations for the amplitudes $V_1(y)$ (See Appendix A). Assuming that V_1 is a slowly varying function of y, one has :

$$\frac{dV_1}{dy} + i\beta_1 V_1 = -\frac{1}{2} i \xi (V_{1+1} + V_{1-1}) \ , \qquad (4)$$

where :

$$\beta_1 = \frac{2 1 k K (\frac{v}{c'} - \operatorname{sen}\theta_o) - 1^2 K^2 (1 - \frac{v^2}{c'^2})}{2 k \cos\theta_o} \ ,$$

$$\xi(y) = \frac{k}{2\cos\theta_o} \frac{\delta\varepsilon}{\varepsilon_o} = \frac{k_o}{\cos\theta_o} \Delta n(y) \qquad (\text{since } \varepsilon_o = n^2) \ , \qquad (5)$$

$$k_o = k/n = \omega/c \ .$$

The initial conditions are $V_1(0) = 0$ for $1 \neq 0$, $V_o(0) = \bar{V}_o$. Equation (4) can be integrated to yield

$$V_1(y) = e^{-i\beta_1 y} \int_0^y dy' \left\{ -\frac{i}{2} \xi(y') \left[V_{1+1}(y') + V_{1-1}(y') \right] \right\} e^{i\beta_1 y'} \qquad (6)$$

where

$$\beta_1 L = 1\beta_1 L + 1(1 - 1)\frac{K^2}{k} L \left(1 - \frac{v^2}{c'^2}\right) \frac{1}{2\cos\theta_o} \qquad (7)$$

Inspection of eqs. (6) and (7) indicates that (see Appendix B) :

a) All the V_1 will be essentially zero unless $\beta_1 L \lesssim \pi$. An exception may hold when ξ is a rapidly varying periodic function of y. This exception is of no interest here, since it corresponds to a situation where the acoustic beam has components moving at large angle relative to the x-axis.

b) When $\beta_{\pm 1} L < \pi$ two cases are possible ; the first occurs when $K^2 L/k < \pi$, and this allows the existence of n diffraction orders till $\beta_n L > \pi$. This is called Raman-Nath regime. The other

case corresponds to $K^2L/k > \pi$ and so only $\beta_{+1} L < \pi$. Hence only the first diffraction order V_{+1} (or V_{-1}) does not vanish. This is called Bragg regime.

1. 2. - Bragg diffraction ($K^2L/k > \pi$).

The quantity $\beta_{\pm 1}$ can be evaluated as a function of θ_o from (5), which yields:

$$\beta_{\pm 1} = \pm K \frac{\operatorname{sen}\theta - \operatorname{sen}\theta_o}{\cos\theta_o} \quad , \tag{8}$$

where θ is an angle defined as:

$$\operatorname{sen}\theta = \frac{v}{c'} \pm \frac{1}{2} \frac{K}{k} \left(1 - \frac{v^2}{c'^2}\right) \quad . \tag{9}$$

The upper sign corresponds to $l = +1 (\theta_+)$, while the lower sign is for $l = -1 (\theta_-)$. If v/c' were zero, θ would be exactly equal to the Bragg angle for scattering off the acoustic wavefront. The parameter $\beta_{\pm 1}$ signifies how close is the scattering to the Bragg condition $\theta_o = \theta$.

Let us calculate the scattering efficiency in the Bragg conditions when ξ is constant:

$$\xi(y) \begin{cases} = \xi & \text{for } 0 \le y \le L \\ = 0 & \text{elsewhere .} \end{cases} \tag{10}$$

Eq. (4) can be written for $l = 0$ and $l = 1$ dropping V_{-1} and V_{+2}:

$$\frac{dV_o}{dy} = -\frac{1}{2} i \xi V_1 \quad , \qquad \frac{dV_1}{dy} + i\beta_1 V_1 = -\frac{1}{2} i \xi V_o \quad . \tag{11}$$

By imposing the boundary conditions:

$$V_o(0) = \bar{V}_o \; ; \qquad \left.\frac{dV_o}{dy}\right|_{y=0} = 0 \; ,$$

$$V_1(0) = 0 \; ; \qquad \left.\frac{dV_1}{dy}\right|_{y=0} = 0 \; , \tag{12}$$

one obtains:

$$V_o(y) = \bar{V}_o \left(\cos\frac{1}{2}\sqrt{\xi^2 + \beta_1^2}\, y + \frac{i\beta_1}{\sqrt{\xi^2 + \beta_1^2}} \operatorname{sen}\frac{1}{2}\sqrt{\xi^2 + \beta_1^2}\, y\right) e^{-\frac{1}{2}\beta_1 y} \quad , \tag{13}$$

$$V_1(y) = -i\xi \bar{V}_o \frac{\operatorname{sen}\frac{1}{2}\sqrt{\xi^2 + \beta_1^2}\, y}{\sqrt{\xi^2 + \beta_1^2}} e^{-\frac{1}{2}\beta_1 y} \quad . \tag{14}$$

When $\theta_o = \theta_+$, β_1 vanishes and the scattering efficiency η turns out to be:

$$\eta = \left|\frac{V_1(L)}{V_o(0)}\right|^2 = \operatorname{sen}^2 \frac{1}{2} \xi L = \operatorname{sen}^2 \bar{\eta}^{1/2} \quad , \tag{15}$$

where $\bar{\eta}$ is the approximated scattering efficiency for low acoustic intensity ($\xi L \ll 1$).

Reminding that[5]:

$$\xi = \frac{k_o \Delta n}{\cos \theta_o} \quad ; \quad \Delta n = \frac{1}{2} n^3 p s \; ; \quad k_o = 2\pi/\lambda_o \; ; \quad P_a = \frac{1}{2} \varrho v^3 s^2 LH \; ,$$

where:

λ_o = free-space optical wavelength,
s_o = steady-state acoustic strain wave amplitude,
p = photoelastic constant,
ϱ = mass density of the medium,
H = acoustic beam haight ,

$\bar{\eta}$ comes out to be:

$$\bar{\eta} = \frac{1}{2} \pi^2 \frac{n^6 p^2}{\varrho v^3} (\lambda_o^2 H \cos^2 \theta)^{-1} P_a L \; . \tag{16}$$

2. - THE CAVITY-DUMPING TECHNIQUE. -

2.1. - Description of the system.

Figure 3 illustrates a folded cavity with an internal acousto-optic modulator. M_1, M_2 and M_3 are highly reflecting mirrors, PT is a total reflection prism, P a prism for the selection of the wavelength and TL is the laser tube.

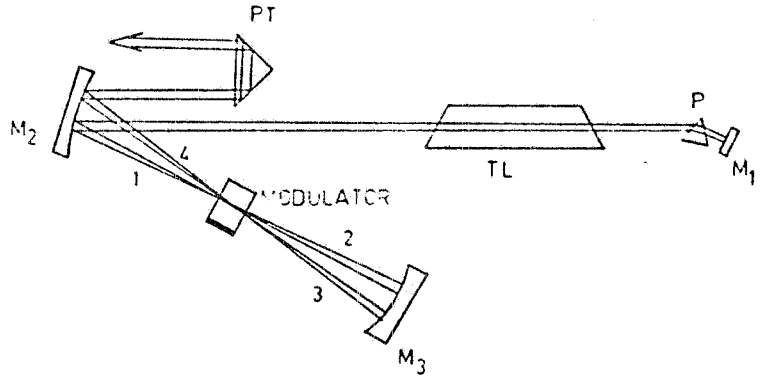

FIG. 3 - Arrangement for the cavity-dumping operation.

The optical dimensioning of this cavity must satisfy some requests:

a) The dimension of the beam in the laser tube must be such to fully use the active medium.

b) There must be in the modulator a waist little enough to achieve the desired rise-time of the scattered light pulses (see later).

c) The distance between the modulator and M_3 must be equal to the curvature radius of M_3.

These requests are achieved with the following values:

$R_1 = \infty$, $R_2 = 20$ cm , $R_3 = 10$ cm ,

Distance between M_1 and M_2 $\simeq$ 127 cm ,

Distance between M_2 and M_3 $\simeq$ 20 cm .

With these values the waist w_o inside the modulator can be calculated according to the matrix method[6] and turns out to be $w_o \simeq 25\ \mu$. With reference to Fig. 3, we determine the power and the frequency composition of the diffracted beam produced by the interaction of the light with the acoustic wave travelling in the modulator.

The beam 1 impinges on the modulator at the Bragg angle θ_-, and therefore, called P its power and ω its frequency, part of it is diffracted in the beam 3 with power ηP and frequency $\omega - \Omega$, where η is the scattering efficiency and Ω the acoustic frequency. The beam 2, that has power $P(1 - \eta)$ and frequency ω, impinges on the modulator at θ_+ and so the output beam 4 has a component with $\eta(1 - \eta)P$ and $\omega + \Omega$. The beam 3, since the modulator is located at the center of curvature of M_3, is reflected back to the modulator and a part with $\eta(1 - \eta)P$ and $\omega - \Omega$ of it goes in the beam 4. Then the output beam, being composed by two parts of equal power $\eta(1 - \eta)P$ and frequency $\omega - \Omega$ and $\omega + \Omega$, has average power $2\eta(1 - \eta)P$ and is 100% modulated at twice the acoustic frequency. We define an overall scattering efficiency η' given by:

$$\eta' = 2\eta(1 - \eta) \ . \tag{17}$$

It can be easily seen that the maximum value for η' is 0.5 corresponding to $\eta = 0.5$. So no more than half of the inside light power can be extracted at each pass. However the arrangement described has the advantage of enhancing the output power stability: for example, as η varies from 0.3 to 0.5, η' goes only from 0.42 to 0.5.

2.2. - Description of the deflector.

The acousto-optic deflector is composed of a substrate of piezoelectric material deposed on a face of a block of fused quartz. The ultrasonic wave produced in the piezoelectric transducer is launched in the quartz and here interacts with the laser beam. The type of the wave generated can be longitudinal or shear, depending upon the transducer material and the orientation of its crystalline axis relative to the applied electric field. In our case the acoustic wave is longitudinal.

It was shown by Maydan[7] that the risetime of the deflected light pulses depends upon the ratio a of the diffraction angles of the light and acoustic waves. The dependence is shown in Fig. 4, where:

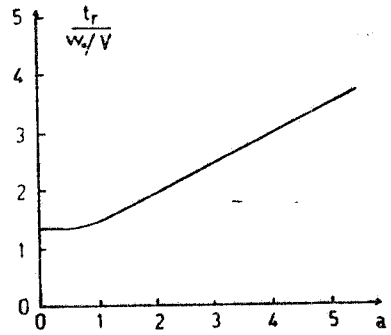

FIG. 4 - Pulse risetime versus the ratio of the diffraction angles.

$$a = \frac{\partial \phi}{\partial \theta} \ , \tag{18}$$

with:

$\partial \phi = \lambda_o / n\pi w_o$,

$\partial \theta = \Lambda / 2L$,

n = refraction index of quartz,

Λ = acoustic wavelength,

L = length of the interaction region.

The risetime t_r is expressed in terms of half the transit time of the acoustic wavefront, having velocity V, across the waist w_o.

In our case the parameters have the values:

$$\lambda_o = 5145\ A^o, \quad n \simeq 1.46, \quad V = 6 \times 10^5\ cm/sec, \quad w_o \simeq 25\mu, \quad F = \Omega/2\pi = 435\ MHz,$$

and consequently we have $a \simeq 1.5$ and from Fig. 4:

$$t_r \simeq 1.7\ w_o/V \simeq 7\ nsec \ .$$

2.3. - Description of the driver.

The piezoelectric transducer of the deflector is commanded by an RF generator at 435 MHz. This value of the acoustic frequency allows to achieve a separation between the diffracted and the undiffracted beam on M_2 given by:

$$s \simeq l \, \lambda_o/\Lambda \simeq 4 \text{ mm},$$

where l is the distance between M_2 and the modulator and λ_o/Λ (see Sect. 1) is the deflection angle.

The RF driver is triggered by the pulses of an external pulse generator giving the start and duration of the RF bunches (Fig. 5). Of course the driver has its own risetime and so the RF bunches are always longer than the generator pulses. In Fig. 6 is shown the base and half-maximum duration of the RF bunches versus the duration τ of the input pulses. The measure was made at a repetion frequency of ~8.5 MHz (T = 1/f ≃ 117 nsec) and keeping constant the average acoustic power.

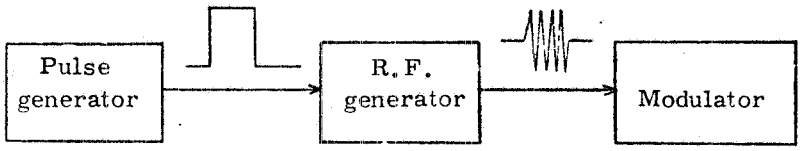

FIG. 5 - Sketch of the modulator driving system.

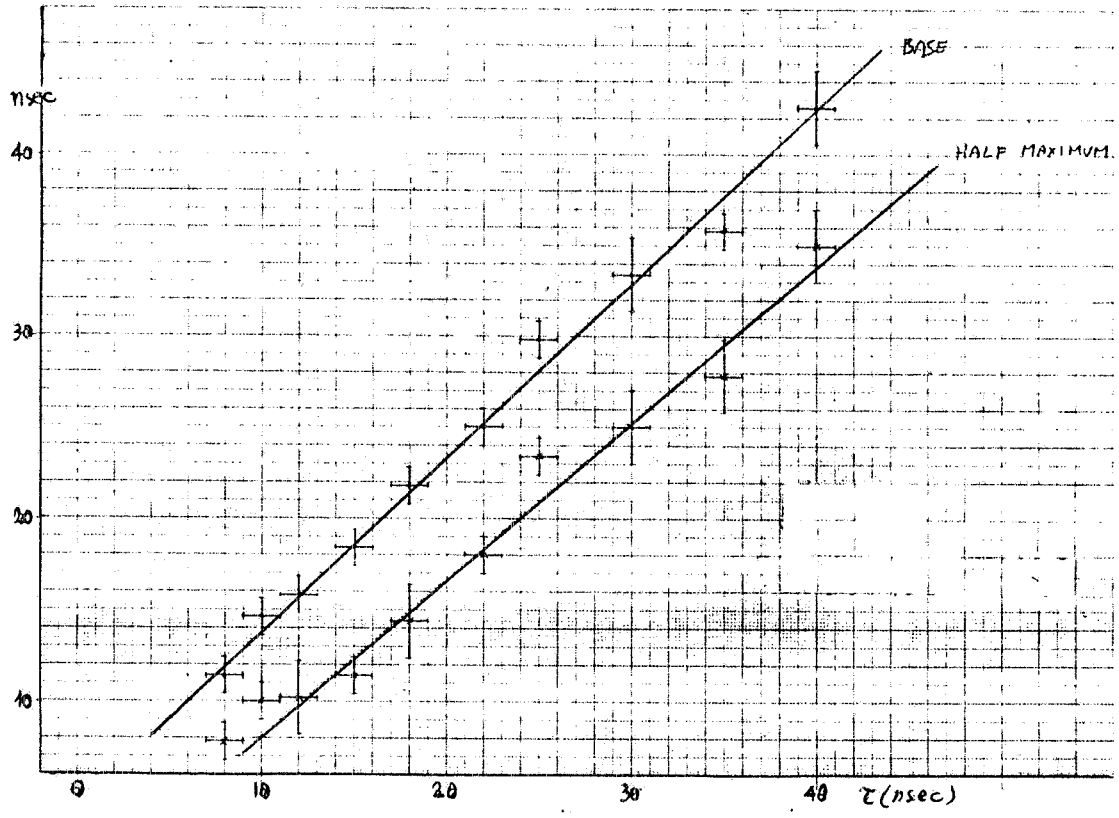

FIG. 6 - Base and half maximum durations of the RF bunches versus the driving pulse duration.

3. - EXPERIMENTAL RESULTS. -

3.1. - Experimental setup.

The laser we used was an Argon ion laser (Spectra Physics mod. 166) which gives an output power of about 2.5 Watts across a semireflecting mirror (4%), at the wavelength $\lambda = 5145$ Å. The cavity dumper was the Spectra Physics mod. 365 acoustooptic output coupler.

According to the type of measure we performed, the output pulsed laser beam was directed to a light power meter to measure the average power or to a fast photodiode to see on an oscilloscope the shape of the light pulses. A slow photodiode mounted behind the flat mirror of the cavity (M_1 of Fig. 3) allows us to measure the inner average power.

3.2. - Measurements.

As explained in the introduction, we produced a train of light pulses with duration less than 20 nsec and studied the behaviour of the device and at repetition period of 117 nsec and also double or triple (234 and 351 nsec). Finally, we measured the total scattering efficiency versus the RF voltage.

The parameters we could vary were:
- the repetition period (T);
- the durations of the pulses driving the RF generator (τ);
- the average acoustic power (P_a);
- the total scattering efficiency (η').

Not all these parameters are independent: for example, fixing T and τ, the maximum η' that can be obtained is limited by the maximum acoustic power (~ 1 Watt) the transducer can produce without damage.

The different types of measurements can be presented as follows:

a) Scattering efficiency.

The expression of the one-way scattering efficiency η can be written:

$$\eta = \text{sen}^2 k V_p \ , \tag{19}$$

where V_p is the RF peak voltage and k is a constant whose expression can be found from (16) considering that $P_a \propto V_p^2$.

The total scattering efficiency is:

$$\eta' = 2\eta(1 - \eta) \ , \tag{20}$$

and, when the RF is driven in a continous way with constant amplitude, it equals the output coupling, i.e., the ratio of the external to the internal power. For each measure of η' and V_p we determined the constant k. The different values of k we found differed from each other for few percent. Fig. 7 shows η and η' versus V_p assuming for k the mean experimental value $k = 3.2 \times 10^{-2}\ V^{-1}$.

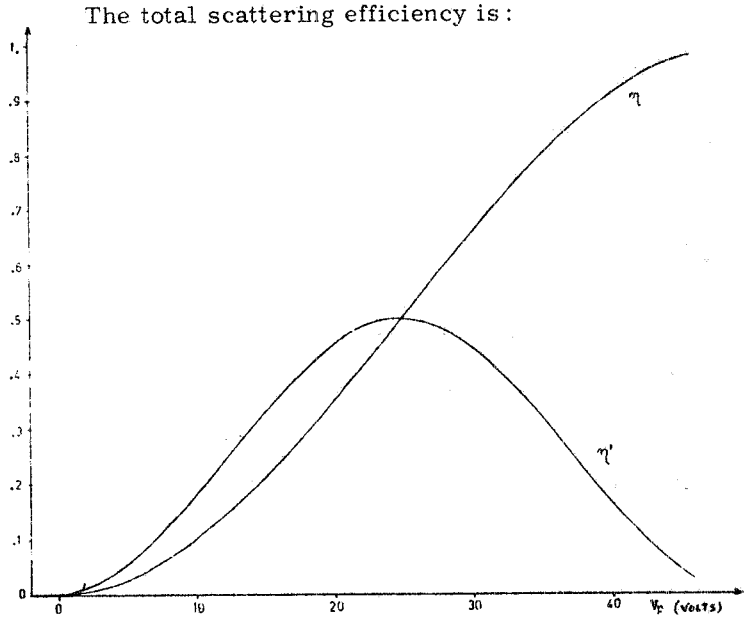

FIG. 7 - One-way (η) and total (η') scattering efficiency versus the RF peak voltage.

b) Pulse shape.

The shape of the light pulses extracted from the cavity has been studied as a function of the duration τ of the driving pulses at a repetition period of 117 nsec ($\sim$ 8.5 MHz). In Fig. 8 are plotted the duration at the base and at half-maximum and the risetime of the light pulse. During this measure the mean acoustic power was kept constant at 1 W. The structure of the light pulses is shown in the oscilloscope photos of Fig. 9. The modulation of the light intensity at twice the acoustic frequency, foreseen in Sec. 2.1, is not 100% due to the oscilloscope cutoff frequency.

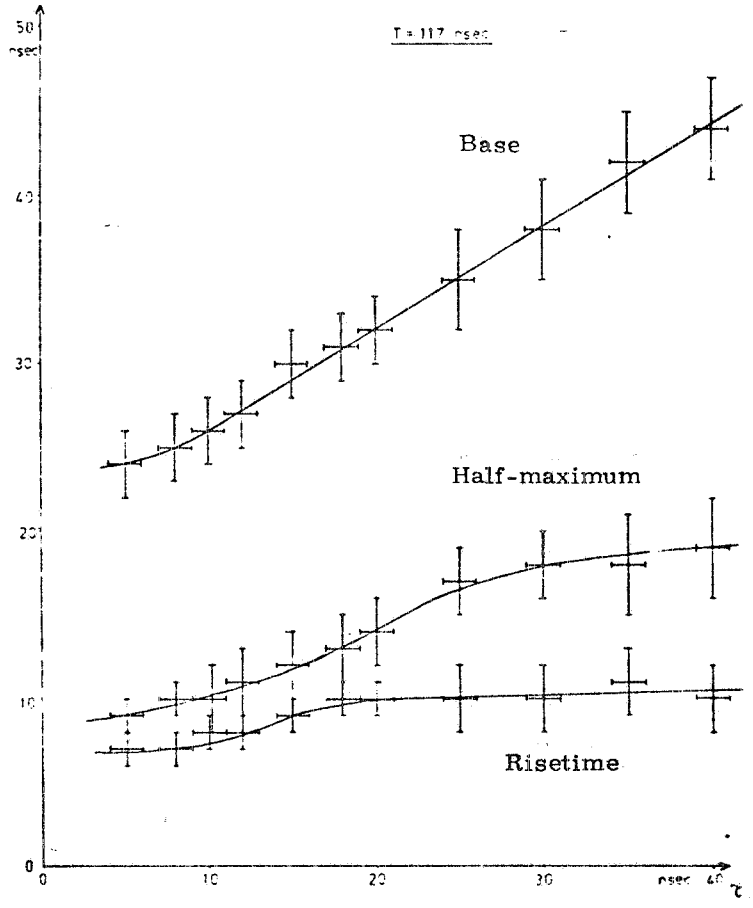

FIG. 8 - Risetime, base and half-maximum duration of the light pulses. Full lines are fit by eyes.

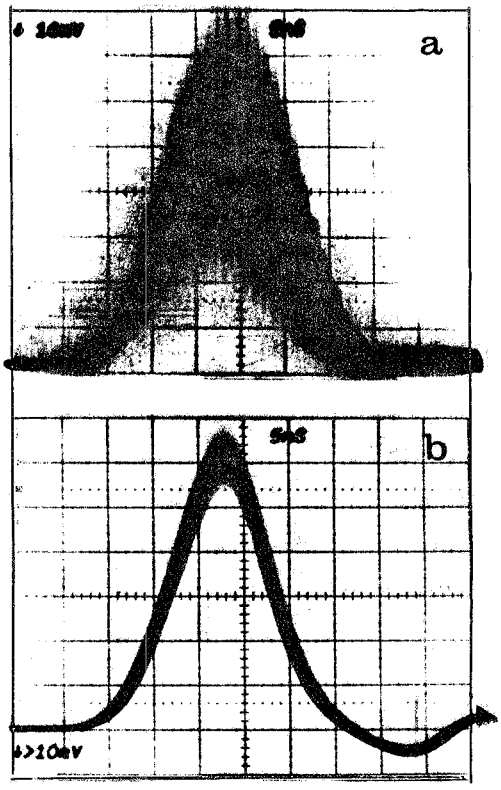

FIG. 9 - a) Light pulse modulation at twice the acoustic frequency (scope cut-off frequency = 500 MHz); b) Light pulse shape (scope cut-off frequency = 200 MHz).

c) Power measurements.

We performed some measurements of the average output power to find its dependence on the duration and repetition period of the driving pulses.

The measure at constant τ and T varying, whose result is reported in Fig. 10, was performed at constant η', while the measure with T constant and τ varying (Fig. 11), at constant P_a. From the last measure we saw that at a given frequency, the average output power has a maximum for a certain value of τ. The optimum value of τ versus the repetition period T at maximum acoustic power is reported in Fig. 12. For an easier interpretation and use of the data, it is better to think of the light pulses as rectangular with duration equal to the half maximum width we measured and height equal to a "peak power" P_p given by:

$$P_p = P_m T/\Delta \ ,$$

where P_m is the average power, T the repetition period and Δ the assumed duration. By using

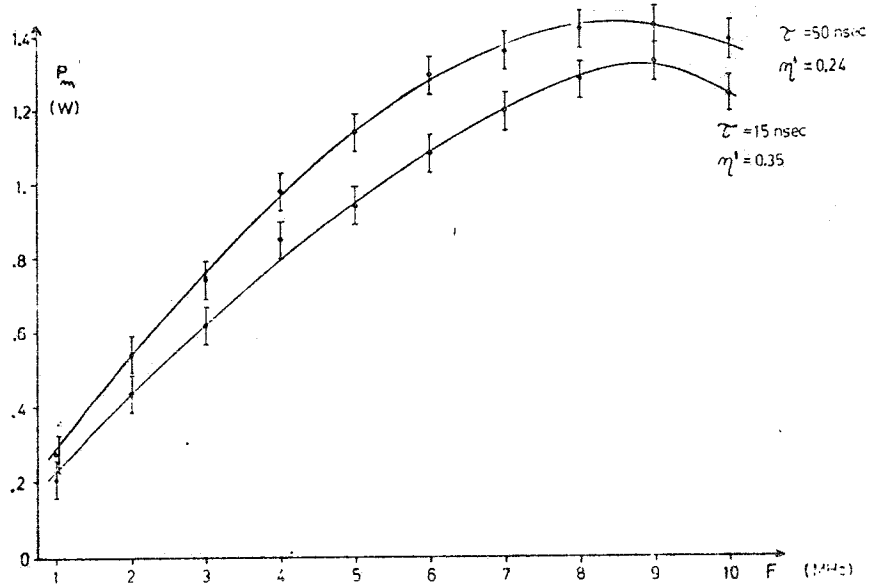

FIG. 10 - Average output power in function of the repetition frequency F, for two values of the driving pulse duration and scattering efficiency. Full lines are fit by eyes.

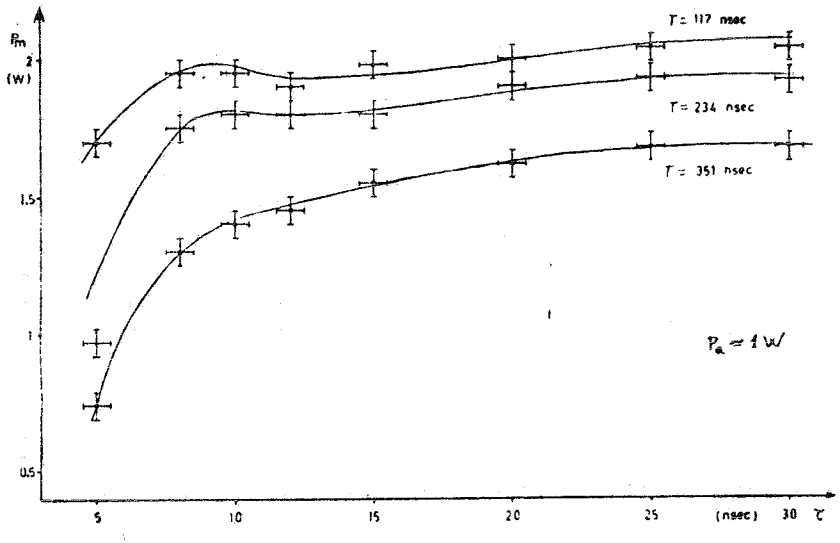

FIG. 11 - Average output power in function of the driving pulse duration at three different repetition periods. Full lines are fit by eyes.

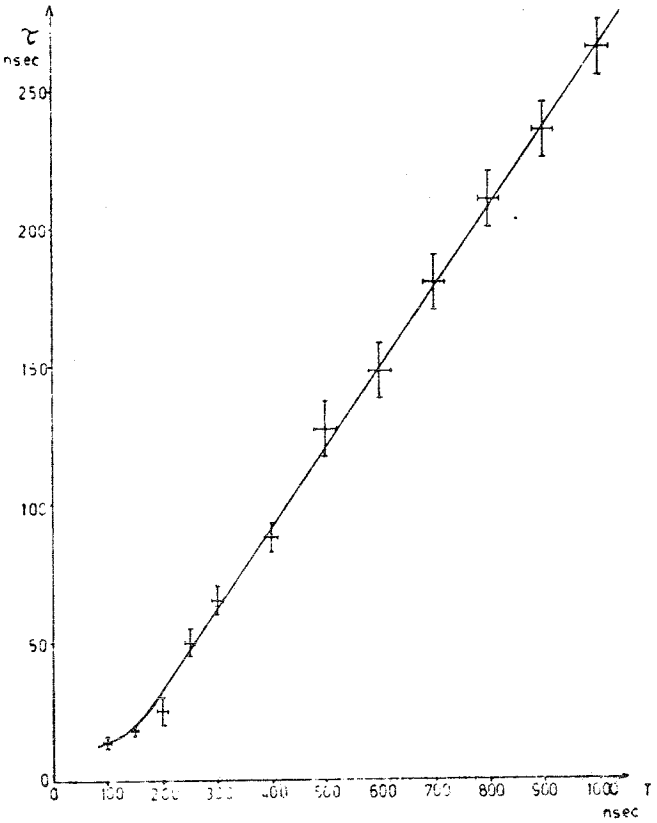

FIG. 12 - Optimum duration versus repetition period. Full line is fit by eyes.

the graphs of Figs. 10 and 7 we reported in Fig. 13 the peak power versus τ at two different repetition frequencies.

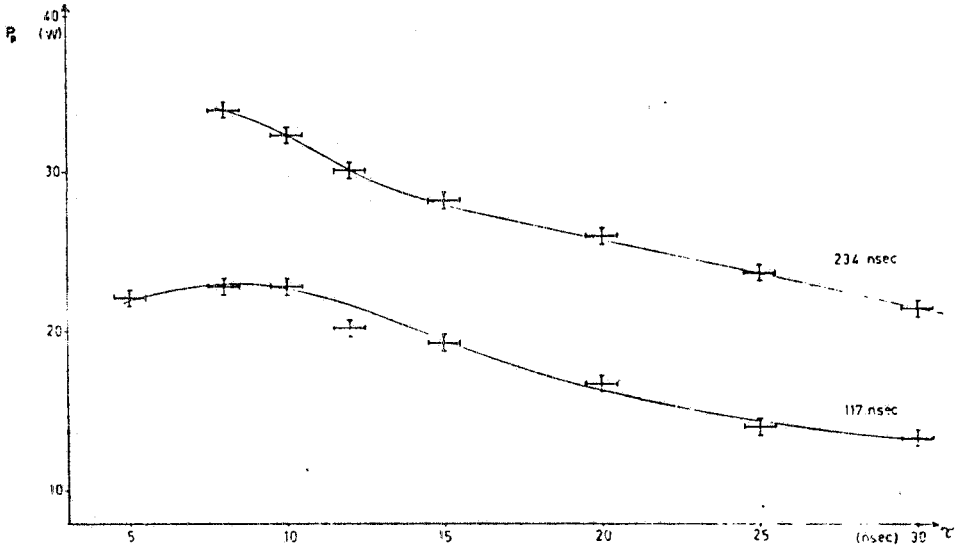

FIG. 13 - Peak power of the light pulses versus their duration at two different frequencies. Full lines are fit by eyes.

4. - DISCUSSION AND COMPARISON WITH THEORY.

In this section we shall discuss the obtained experimental results by comparing them with the theoretical expectations of Section 1.1. In addition, a brief summary of the saturation effects of the laser gain will complete the theoretical framework of the analysis.

4.1. - Gain saturation in lasers.

The natural width of the laser transition is broadened in a laser tube by two principal kinds of effects: the interaction between the atoms of the active medium ("homogeneous-type broadening") and the Doppler effect rising from the thermal movements of the atom ("inhomogeneous-type broadening").

We can define in both cases a gain curve $g(\nu - \nu_o)$ expressing the gain experienced by a light beam of frequency ν near the central transition frequency ν_o after it has gone a unit length of active medium. The saturation effect of the gain consists of a decrease of gain with the increase of the light power density. We can treat this effect defining first a gain curve $g_o(\nu - \nu_o)$ for light beams with power density tending to zero.

The gain curve $g_o(\nu - \nu_o)$ has a Lorentzian or Gaussian shape according to whether the broadening is homogeneous or inhomogeneous[8]:

$$g_o(\nu - \nu_o) = g_o(\nu_o)\left[1 + \left(\frac{\nu - \nu_o}{\Delta\nu}\right)^2\right]^{-1} \qquad \text{(homogeneous)},$$

$$g_o(\nu - \nu_o) = g_o(\nu_o)\exp\left[-\left(\frac{\nu - \nu_o}{\Delta\nu}\right)^2\right] \qquad \text{(inhomogeneous)}.$$

When the light beam crossing the active medium has a non-zero density power the gain curves suffer a modification.

In the homogeneous case the shape of the gain curve does not change but its height becomes a $g_h(P)$ given by[9]:

$$g_h(P) = g_o\left[1 + P/P_m\right]^{-1} ,$$

where P is the light density power and P_m a saturation parameter. Then, in the case of homogeneous broadening the presence of light at frequency ν changes the gain at all frequencies. On the contrary, in the inhomogeneous case, it changes the gain only at the same frequency ν. In this case the gain in correspondence of each oscillating frequency is given by[9]:

$$g_{inh}(P) = g_o\left[1 + P/P_m\right]^{-1/2} .$$

This difference between the two types of broadening can be explained as follows: in the homogeneous case all the atoms of the active medium emit in a same broadened line, so a light beam of any frequency can induce transitions with any of them and with the same probability. Hence the presence of light at some frequency ν changes the gain at all frequencies. On the contrary, in the inhomogeneous case any atom emits with the natural linewidth at a frequency depending on its velocity; so a light beam of frequency ν can induce the stimulated emission only in those atoms having a certain velocity component in the light propagation direction. Therefore two light beams with different frequencies, can interact only with different groups of atoms and consequently experience a gain not influenced by the presence of the other ones.

The interval power of a laser cavity is, in static conditions, such that the gain equals the sum a of the internal and output losses for single pass

$$g_o L\left[1 + P_{int}/P_m\right]^{-\nu} = a ,$$

(ν = 1 or 1/2, L is the active medium length) and then :

$$P_{int} = P_m\left[(g_o L/a)^{1/\nu} - 1\right] . \qquad (21)$$

If at any instant, the internal power has not the steady-state value given by (21), its changing in function of time is expressed by the differential equation[10]:

$$\frac{dP}{dt} = \frac{P}{L'/c}\left[\frac{g_o L}{(1 + P/P_m)^{\nu}} - a\right] , \qquad (22)$$

where L' is the cavity length and c is the velocity of light. Eq. (22) can be integrated to yield in the homogeneous case[10] (ν = 1):

$$\frac{1}{g_o L}\log\left(\frac{g_o L}{L'/c}\ \frac{\beta}{\beta_s}\right) - \frac{1}{a}\log\left[\frac{g_o L}{L'/c}\left(1 - \frac{\beta}{\beta_s}\right)\right] = \frac{t}{L'/c} , \qquad (23)$$

with the boundary conditions: $\beta \to 0$ for $t \to -\infty$ and $\beta \to \beta_s$ for $t \to +\infty$; where β and β_s are the instantaneous and steady-state powers normalized to the saturation parameter P_m ($\beta = P/P_m$). We can define a recovery time as the time required for the internal power to go from 10% to 90% os its steady-state value. The recovery time τ_r is now :

$$\tau_r \simeq 2.2\,\frac{L'}{c}\left(\frac{1}{a} + \frac{1}{g_o L}\right) .$$

In the inhomogeneous case ($\nu = 1/2$), the integration of (22) yields, with the same boundary conditions :

$$\frac{a}{\beta_s}\left\{\log\beta - (\beta_s+1)^{\frac{1}{2}}\log\frac{(1+\beta)^{\frac{1}{2}}+1}{(1+\beta)^{\frac{1}{2}}-1} - 2(\beta_s+1)\log\left[(1+\beta_s)^{\frac{1}{2}} - (1+\beta_s)^{\frac{1}{2}}\right]\right\} = \frac{t}{L'c} \quad . \tag{24}$$

The experimental procedure to determine the parameters $g_o L$, a and P_m of the laser tube was the following: we drove the cavity dumper in a continuous way, so as to assimilate it to a fixed output coupling η', then we measured the outer and internal power and from that we determined η'. Changing the driving voltage of the modulator, we obtained a curve of the internal power versus the "transmittivity" loss η'. Finally we made the fit of this curve with the expression (21): the best fit was obtained for $\nu = 1/2$ (inhomogeneous broadening) and the resulting values of the parameters were :

$$g_o L = 0.284 ,$$
$$a = 0.032 , \qquad \text{(only internal losses)}$$
$$P_m = 1.1 \text{ W} .$$

In the homogeneous case the fit gave a too low value for a. In Fig. 14 are shown the "recovery curves" (23) and (24) with the parameters values given by the fit.

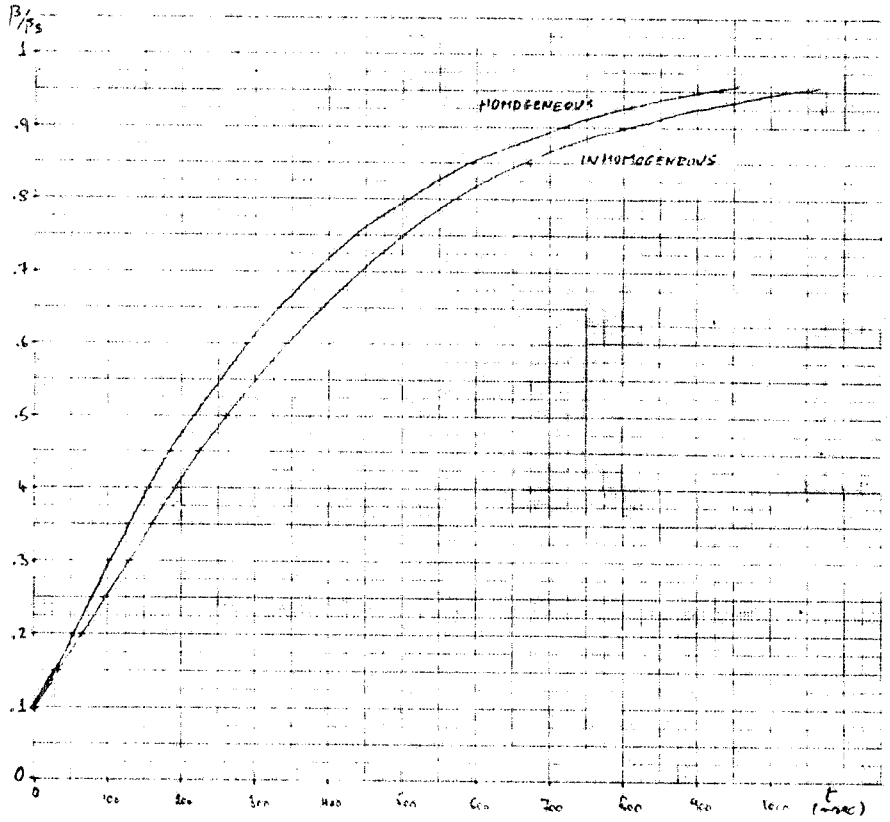

FIG. 14 - Energy recovery curves computed with the following parameters : homogeneous: $g_o L \simeq 0.21$, $a \simeq 0.016$; inhomogeneous : $g_o L \simeq 0.28$, $a \simeq 0.032$.

4. 2. - Discussion of the experimental results.

Let us specialize eq. (22) for the case of the cavity dumper with the inclusion of the exit loss $\eta'(t)$. In the inhomogeneous case, one has:

$$\frac{dP}{dt} = \frac{P}{L'/c}\left[\frac{g_o L}{(1+P/P_m)^{1/2}} - a - \frac{\eta'(t)}{2}\right]. \qquad (25)$$

We have numerically solved eq. (25) by the Runge-Kutta method to get a simulation of the light pulse shape. The value of $\eta'(t)$ was found at any instant as the spatial superposition integral of the gaussian light beam and of the RF bunch moving through it.

In Fig. 15 we have compared a typical light pulse with the shape resulted from our calculations. The values of the parameters used where:

- repetition period = 117 nsec ,
- duration of the driving pulses = 15 nsec ,
- P_m = 1.1 W , $g_o L$ = 0.284 , a = 0.02 , η'_{max} = 0.35 .

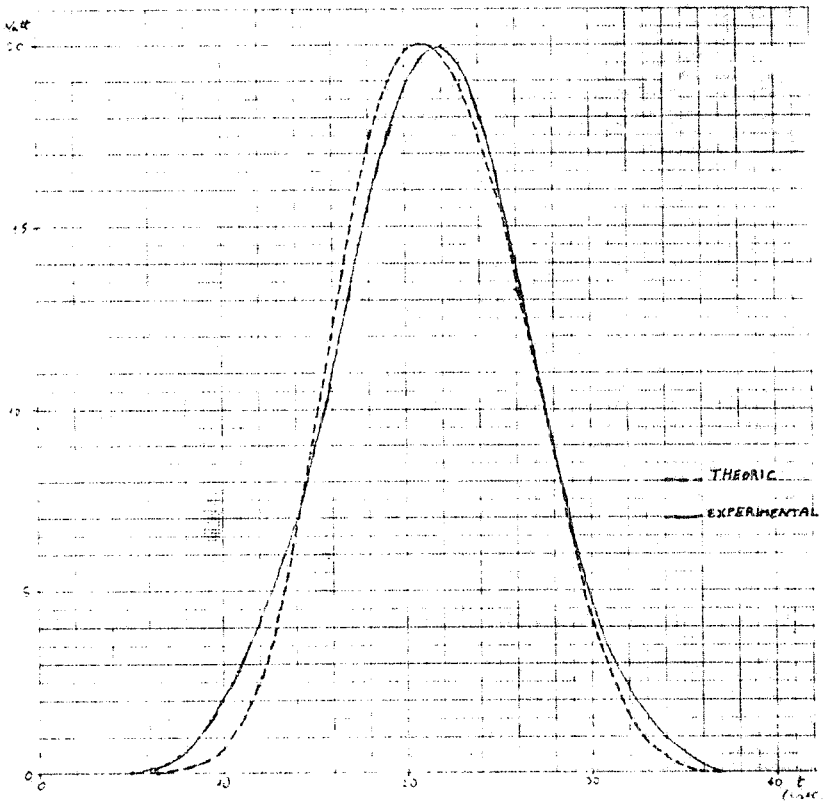

FIG. 15 - Comparison of a typical experimental light pulse shape with the computed one.

We had to fix the internal losses at 2% to have a value of the average output power about equal to the really observed one ($\sim$ 2 W); this means that when we made the measures we used for the fit, the cavity disalignement and the dirtiness of its optical elements were such to lead the losses to a higher value.

As can be seen from Fig. 14, the agreement of our calculations with the experiment is satisfying.

We want now to mention all the approximations and hypothesis we have made up to now:

a) A real active medium is never purely "homogeneous" or "inhomogeneous", but it has a behaviour intermediate between those two extremes, more or less near to one or the other.

b) We have always neglected the existence of more than one oscillating frequency.

c) Eq. (25) assumes that the gain, the internal losses and the output losses are uniformly distribu ted over the cavity length.

5. - CONCLUSIONS : Appliance to the Ladon project. -

The pulsed laser beam obtained with the cavity-dumping technique satisfies the requests il lustrated in the introduction for its use in the Ladon project. In fact, the duration of the light pul ses can be made shorter than 20 nsec, such to avoid the interaction with the electrons in the qua drupole zones ; their repetition period can be made equal to the time interval between two elec- trons bunches by triggering, with an adjustable delay, the pulse generator with an appropriate signal from Adone itself.

The dimensions of the laser beam inside the straight section is little enough to achieve a good superposition with the electron bunch. In fact, as shown in Fig. 16, the laser beam return ing from the mirror has in the straight section a mean radius about 1 mm (at $1/e^2$ points), while the dimensions of the electron bunch is there 0.75 mm in the horizontal plane and 0.25 mm ver tically (radii at $1/e^{1/2}$ points).

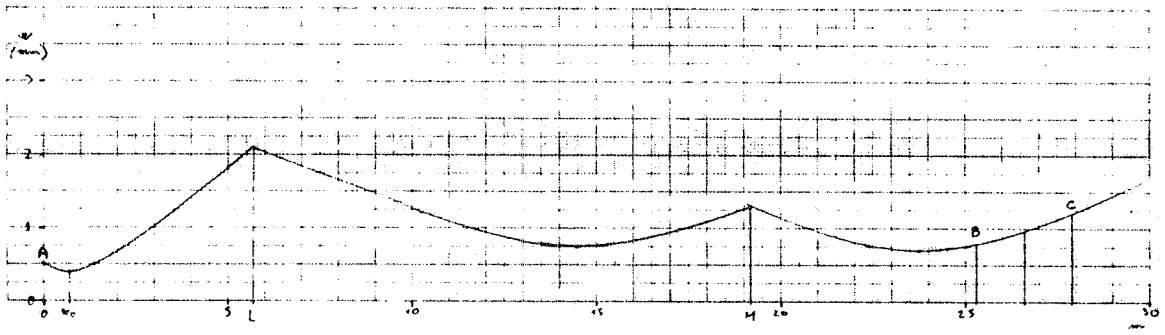

FIG. 16 - Dimension of the laser beam (A : exit from laser ; L : lens with F = 338 cm ; M: mirror with R = 678 cm ; BC : Adone straight section without quadrupoles ; w_o : waist $\sim 4 \times 10^{-2}$ cm at $\sim$70 cm from the exit of laser).

With the reported values for the characteristic parameters of the light pulses (20 W x 15 nsec) an electron current of 100 mA (E_e = 1.5 GeV), and an acceptance solid angle of 10^{-8} ste rad, the expected counting rate comes out to be $\sim 10^5$ γ/sec[11].

REFERENCES.

(1) - R. Caloi et al., Laser light against high energy electron scattering, Frascati report LNF-76/31 (1976); invited contribution to the Europhysics Study Conference on High Power Laser and Scientific Applications, Oxford (1975); Laser and Unconventional Optics Journal 55, 3 (1975).
(2) - G. Matone and A. Tranquilli, Laser light modulation: the electrooptic effect, Frascati report LNF-76/7 (1976).
(3) - B. Gordon and A. R. Cohen, Electrooptic diffraction grating for light beam modulation and diffraction, IEEE J. Q. E. 5, 191 (1965).
(4) - M. Born and E. Wolf, Principles of optics (Pergamon Press, 1975).
(5) - P. Graf, Modulators and deflectors, Alta Frequenza 41, 726 (1972).
(6) - A. Tranquilli, Realizzazione di un fascio gamma monocromatico e polarizzato mediante effetto Compton di luce laser sugli elettroni relativistici circolanti in Adone, Frascati report LNF-75/10 (1975).
(7) - D. Maydan, Acoustooptical pulse modulators, IEEE J. Q. E. 6, 15 (1970).
(8) - O. Svelto, Principi di laser (Tamburini, 1972).
(9) - W. W. Rigrod, Gain saturation and output power of optical masers, Journ. Appl. Phys. 34, 2602 (1963).
(10) - D. Maydan, Fast modulator for extraction of internal laser power, Journ. Appl. Phys. 41, 1552 (1970).
(11) - G. Matone, in Photonuclear Reactions II - Intern. School on electro and photonuclear reactions (Erice, 1976) (Edited by S. Costa and C. Schaerf) (Springer, 1977), pag. 149.

APPENDIX A. - Recurrence relations for $V_l(y)$.

The expression (3) sec. 1.1 for the optical electric field $E(x,y,t)$ is:

$$E(x,y,t) = \sum_{-\infty}^{+\infty}{}_l \; V_l(y) \exp i\left[(\omega + l\Omega)t - (k \operatorname{sen}\theta_o + lK)x - k\cos\theta_o y\right] + \text{C.C.} \qquad \text{(A.1)}$$

The y-component of the light wave-vector $\vec{k}$ is the same for all the diffraction orders since the acoustic wave-vector $\vec{K}$ has been assumed to have only the x-component.

By substituting (A.1) in eq. (2) sec. 1.1. one has:

$$\sum_{-\infty}^{+\infty}{}_l \left\{ V_l(y)\left[\frac{\omega_l^2}{c'^2} - k_l^2 - h^2\right] - 2ihV_l'(y) + \frac{\Omega^2+\omega_l^2}{c'^2}\,\delta\varepsilon(y)\cos(\Omega t - Kx)\,V_l(y) + \right.$$

$$\left. + 2i\,\frac{\omega_l \Omega}{c'^2}\,\delta\varepsilon(y)\operatorname{sen}(\Omega t - Kx)\,V_l(y)\right\} e^{ia(l)} + \text{C.C.} = 0 \;, \qquad \text{(A.2)}$$

where:

$$a(l) = (\omega + l\Omega)t - (k \operatorname{sen}\theta_o + lK)x - k\cos\theta_o y \;,$$

$$\omega_l = \omega + l\Omega \;,$$

$$k_l = k \operatorname{sen}\theta_o + lK \;,$$

$$h = k\cos\theta_o \;.$$

Terms in $V_l''(y)$ have been neglected since it has been assumed that $V_l(y)$ is a slowly varying function of y. The last two terms of eq. (A.2) can be arranged as follows:

$$\sum_{-\infty}^{+\infty}{}_l \frac{1}{c'^2}\,\delta\varepsilon(y)\,V_l(y)\left\{(\Omega^2+\omega_l^2)\cos(\Omega t - Kx) + 2i\Omega\,\omega_l \operatorname{sen}(\Omega t - Kx)\right\}\left\{\cos a(l) + i \operatorname{sen} a(l)\right\} =$$

$$= \sum_{-\infty}^{+\infty}{}_l \frac{V_l(y)}{c'^2}\,\frac{\delta\varepsilon(y)}{2}\left[\omega_{l+1}^2\, e^{ia(l+1)} + \omega_{l-1}^2\, e^{ia(l-1)}\right] =$$

$$= \frac{\delta\varepsilon(y)}{2c'^2}\left\{\sum_{-\infty}^{+\infty}{}_j V_{j-1}(y)\,\omega_j^2\, e^{ia(j)} + \sum_{-\infty}^{+\infty}{}_k V_{k+1}(y)\,\omega_k^2\, e^{ia(k)}\right\} =$$

$$= \frac{\delta\varepsilon(y)}{2c'^2}\sum_{-\infty}^{+\infty}{}_l\, \omega_l^2\left[V_{l+1}(y) + V_{l-1}(y)\right] e^{ia(l)} \;.$$

Eq. (A.2) is then:

$$\sum_{-\infty}^{+\infty}{}_l \left\{\left(\frac{\omega_l^2}{c'^2} - k_l^2 - h^2\right)V_l(y) - 2ihV_l'(y) + \frac{\delta\varepsilon(y)}{2c'^2}\,\omega_l^2\left[V_{l+1}(y) + V_{l-1}(y)\right]\right\} e^{ia(l)} + \text{C.C.} = 0 \;,$$

and can be put in the following form:

$$\sum_{-\infty}^{+\infty}{}_l \left(F_l\, e^{ia(l)} + F_l^*\, e^{-ia(l)}\right) = 0 \;. \qquad \text{(A.3)}$$

A solution of eq. (A. 3) can be found by setting

$$\sum_{-\infty}^{+\infty} {}_1 F_1 \, e^{ia(1)} = 0 \qquad (A.4)$$

since a set of $V_1(y)$ satisfying (A. 4), satisfies also (A. 3). Now, the $e^{ia(1)}$ are a set of linearly independent functions, and therefore condition (A. 4) is equivalent to put all the F_1 equal to zero. This drives to the relation:

$$\left(\frac{\omega_1^2}{c'^2} - k_1^2 - h^2\right) V_1(y) - 2ih V_1'(y) + \frac{\delta\varepsilon(y)}{c'^2} \omega_1^2 \left[V_{1+1}(y) + V_{1-1}(y)\right] = 0 ,$$

that is identical to eq. (4) sec. 1. 1.

APPENDIX B. - Conditions on the β_1.

Let us rewrite eqs. (6) and (7) sec. 1. 1 :

$$V_1(y) = e^{-i\beta_1 y} \int_0^y dy' \left\{ -\frac{i}{2} \xi(y') \left[V_{1+1}(y') + V_{1-1}(y')\right] \right\} e^{i\beta_1 y'} , \qquad (B.1)$$

$$\beta_1 L = 1\beta_1 L + 1(1-1) \frac{K^2}{k} L \left(1 - \frac{v^2}{c'^2}\right) \frac{1}{2\cos\theta_o} . \qquad (B.2)$$

Some qualitative information on the amplitudes $V_1(y)$ can be obtained with the following simple reasoning.

If $\xi(y)$ and the $V_1(y)$ are slowly varying functions of y, as it is almost always verified, the integral in (B. 1) is essentially zero if the length L of the interaction region is equal or greater than half a period of the oscillating function $e^{i\beta_1 y}$, that is if

$$|\beta_1 L| \gtrsim \pi . \qquad (B.3)$$

Moreover, from (B. 2) $\beta_1 L$ can be expressed as :

$$\beta_1 L = 1A - 1^2 B , \qquad (B.4)$$

which is a parabola with its concavity downward and passing through the origin.

The case a) sec. 1. 1 is with $(A-B) > \pi$ ($\beta_1 L > \pi$), and, as shown in Fig. 17a the parabola crosses the strip $(-\pi, +\pi)$ in an interval of 1 less than 2, so there is essentially only one value $\bar{1}$ for which $\beta_{\bar{1}} L < \pi$. But $V_{\bar{1}+1}$ and $V_{\bar{1}-1}$ are zero because $\beta_{\bar{1}+1} L > \pi$ so also $V_{\bar{1}}$ is zero, even if $\beta_{\bar{1}} L < \pi$. This explains what we asserted in a) sec. 1. 1.

The first case of b) sec. 1. 1 corresponds to $(A-B) < \pi$ and $B < \pi$ (Raman-Nath regime). Now the parabola has a certain interval of 1 for which $\beta_1 L < \pi$ (Fig. 17b), so more than one sideband can exist.

The second case is with $(A-B) < \pi$ and $B > \pi$ (Bragg regime). The situation is shown in Fig. 17c where $\beta_{-1} L$ and $\beta_2 L$ are already less than $-\pi$, so that only V_1 can exist.

We have always discussed in terms of β_{+1}, but all our reasonings can be exactly repeated in terms of β_{-1}.

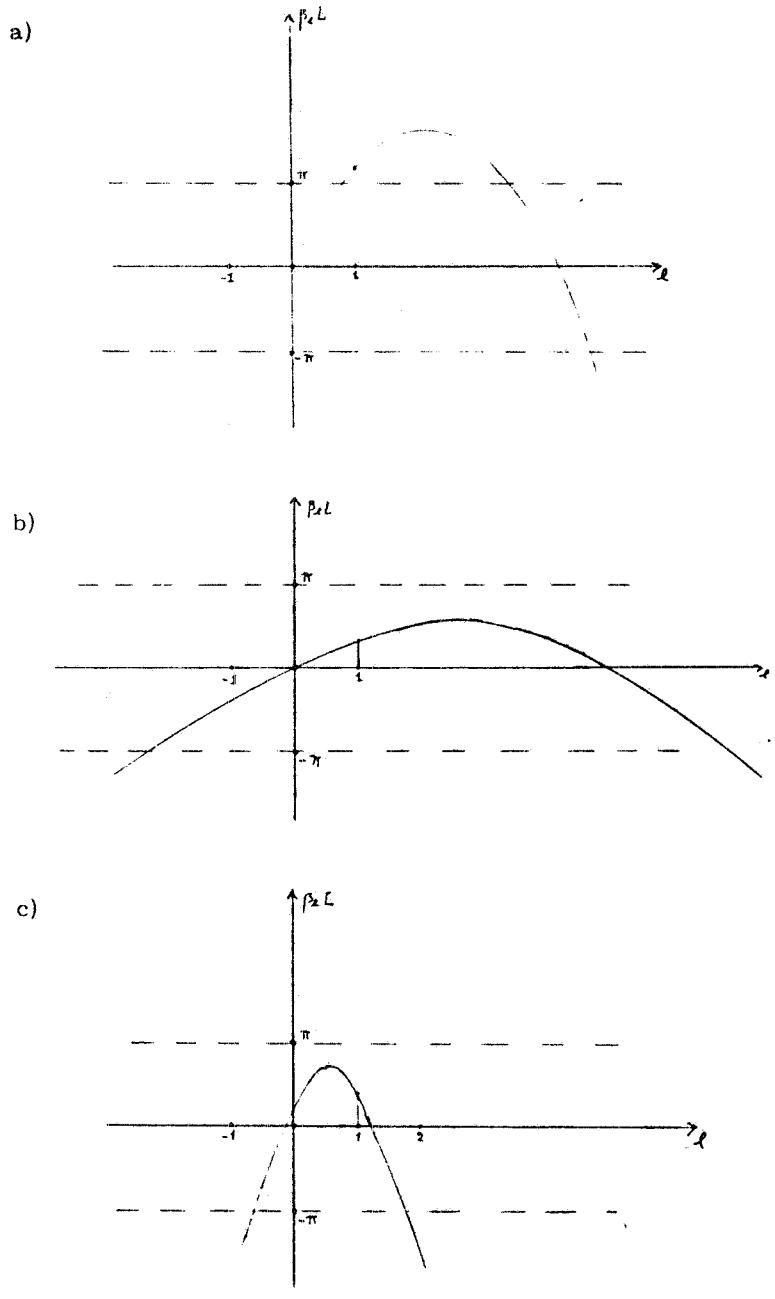

FIG. 19 - a) $\beta_1 L > \pi$. No sidebands existing.

b) $\beta_1 L < \pi$, $K^2 L/k < \pi$. Raman-Nath regime. Many sidebands existing.

c) $\beta_1 L < \pi$, $K^2 L/k > \pi$. Bragg regime. Only V_{+1} existing.